Geotextiles and Geomembranes 29 (2011) 544–556

Contents lists available at ScienceDirect

Geotextiles and Geomembranes

journal homepage: www.elsevier.com/locate/geotexmem

Consolidation enhanced membrane behavior of a geosynthetic clay liner

Jong-Beom Kang [a,1], Charles D. Shackelford [b,*]

[a] Engineering Analytics[2], Inc., 1600 Specht Point Road, Suite 209, Fort Collins, CO 80525, USA
[b] Department of Civil and Environmental Engineering, 1372 Campus Delivery, Colorado State University, Fort Collins, CO 80523-1372, USA

ARTICLE INFO

Article history:
Received 22 December 2010
Received in revised form
6 June 2011
Accepted 17 July 2011

Keywords:
Bentonite
Consolidation
Geosynthetic clay liner
Membrane behavior
Osmosis
Waste containment

ABSTRACT

Semipermeable membrane behavior in clays refers to the ability of clays to restrict the migration of solutes. Thus, membrane behavior represents a potential benefit to the containment function of clay barriers used for hydraulic containment applications. In this regard, the potential influence of consolidation effective stress, σ', on the membrane behavior of a geosynthetic clay liner (GCL) containing sodium bentonite was evaluated in the laboratory by establishing differences in salt (KCl) concentrations ranging from 3.9 to 47 mM across specimens of the GCL in a flexible-wall cell under closed-system boundary conditions. The membrane behavior exhibited by the GCL was enhanced via consolidation such that an increase in σ' from 34.5 kPa (5 psi) to 241 kPa (35 psi) correlated with an increase in membrane efficiency from 0.015 (1.5%) to 0.784 (78.4%), respectively. The membrane efficiencies measured in this study at σ' of 172 kPa (25 psi) and 241 kPa (35 psi) were similar to those previously reported for the same GCL using a rigid-wall cell but at unknown states of stress. The practical significance of the results is illustrated in the form of an analysis showing a reduction in liquid flux across the GCL with increasing membrane efficiency.

1. Introduction

Geosynthetic clay liners (GCLs) are manufactured hydraulic barriers typically consisting of a thin layer (~5–15 mm) of natural or treated bentonite (sodium or calcium) sandwiched between two geotextiles and/or glued to a geomembrane (Daniel et al., 1993; Koerner and Daniel, 1995; Bouazza, 2002; Koerner, 2005). The primary differences among GCLs are the mineralogy (e.g., content of montmorillonite) and form (e.g., powdery versus granular) of bentonite used in the GCL, the type of geotextile (e.g., woven versus non-woven), the hydration condition (e.g., non-prehydrated versus prehydrated), and the method of bonding the component materials together (e.g., Daniel et al., 1993; Koerner and Daniel, 1995; Shackelford et al., 2000; Lee and Shackelford, 2005).

Prefabricated GCLs are used extensively as barriers or components of barriers designed and constructed for a wide variety of hydraulic containment applications, including landfill liners and covers, surface impoundments (e.g., ponds and lakes, aeration lagoons, fly ash lagoons, and other surface impoundments), canals, storage tanks, and secondary containment of above-grade fuel storage tanks (e.g., Koerner, 2005; Benson et al., 2007, 2010; Bouazza and Vangpaisal, 2007a,b; Lake et al., 2007; Abduel-Naga and Bouazza, 2009, 2010; Guyonnet et al., 2009; Dickinson and Brachman, 2010; Dickinson et al., 2010; Hornsey et al., 2010; Kang and Shackelford, 2010; Lange et al., 2007, 2009, 2010; Mendes et al., 2010a,b; Rossin-Poumier et al., 2010, 2011; Scalia and Benson 2010, 2011; Shackelford et al., 2010). The use of GCLs for hydraulic containment applications has increased over the past decade due to several advantages, including relatively easy installation, resistance to freezing/thawing and wetting/drying cycles (i.e., in the absence of multivalent for monovalent cation exchange), low cost, and low hydraulic conductivity to water (i.e., $<10^{-10}$ m/s) (Estornell and Daniel, 1992; Daniel et al., 1993; Koerner and Daniel, 1995; Boardman and Daniel, 1996; Hewitt and Daniel, 1997; Lee and Shackelford, 2005; Meer and Benson, 2007; Benson and Meer, 2009). In addition, GCLs also have been found to behave as semipermeable membranes, thereby restricting the migration of solutes (Malusis and Shackelford, 2002a,b). Since one purpose of clay barriers used in hydraulic containment applications is to restrict the migration of aqueous miscible contaminants (i.e., solutes), the existence of membrane behavior in GCLs represents a potentially significant beneficial aspect in the use of GCLs for such applications.

* Corresponding author. Tel.: +1 970 491 5051; fax: +1 970 491 7727.
E-mail addresses: jkang@enganalytics.com (J.-B. Kang), shackel@engr.colostate.edu (C.D. Shackelford).
[1] Tel.: +970 488 3111; fax: +970 488 3112.
[2] The author was formerly, Graduate Research Assistant, Department of Civil and Environmental Engineering, Colorado State University, Fort Collins, CO 80523-1372, USA.

0266-1144/$ – see front matter © 2011 Elsevier Ltd. All rights reserved.
doi:10.1016/j.geotexmem.2011.07.002

Membrane behavior in clays is characterized by restricted passage of solutes, as well as by chemico-osmosis, or the movement of water from lower solute concentration (higher water activity) to higher solute concentration (lower water activity) (Shackelford et al., 2003). Restricted passage of electrolytes (anions and cations) occurs when the pore sizes of the clay are sufficiently small such that electrostatic repulsion of the ions results from the interaction of electric fields associated with adjacent clay particles (e.g., Fritz, 1986). In this case, the overlapping negative electrical potentials resulting from the predominantly negative charges of the particle surfaces prevent anions from entering the pore, and the cations within the electrolyte solution are similarly restricted from migration due to the requirement for electroneutrality in solution (Shackelford, 2011).

Membrane behavior is quantified in terms of an efficiency coefficient representing the relative degree of solute restriction. In the science literature, this efficiency coefficient commonly is designated by the symbol, σ, and referred to as the "reflection coefficient". However, the symbol σ in the engineering literature typically is used to represent stress or electrical conductance (e.g., Mitchel and Soga, 2005). As a result, the symbol ω typically is preferred in the engineering literature to represent the "membrane efficiency coefficient". Because membrane behavior also results in chemico-osmosis, ω often is referred to as the "osmotic efficiency coefficient" or the "chemico-osmotic efficiency coefficient", although the latter term is preferred to distinguish chemico-osmosis from other osmotic phenomena, such as electro-osmosis and thermo-osmosis (Shackelford, 2011). The term "membrane efficiency" is a general term referring to the relative extent of solute restriction as given by the value of ω expressed in percent.

In general, the value of ω ranges from zero ($\omega = 0$) in the case where no membrane behavior exists, to unity ($\omega = 1$) in the case where all migrating solutes are restricted. An "ideal" or "perfect" membrane is a membrane that exhibits 100 percent efficiency ($\omega = 1$). In naturally occurring clays that exhibit membrane behavior, a distribution in pore sizes typically exists, such that some of the pores are restrictive but others are not. As a result, the membrane efficiencies of natural clays that exhibit membrane behavior generally range between zero and 100 percent (i.e., $0 < \omega < 1$), and such clays are referred to as "nonideal" or "imperfect" membranes.

The terms "semipermeable", "selectively permeable", "partially permeable", and "differentially permeable" often are used in connection with the existence of membrane behavior (Shackelford, 2011). These terms generally are derived from two possible occurrences. First, the existence of some larger pores in nonideal membranes allows some solutes to migrate through the membrane along with the solvent water molecules (i.e., H_2O). Second, ideal membranes that are 100 percent efficient in terms of restricting solute migration generally are still permeable to the solvent water molecules.

In general, semipermeable membrane behavior in compressible clays is known to increase with decrease in the void ratio of the clays (Shackelford et al., 2003). For example, Olsen (1969) showed that the membrane behavior of kaolin clay could be enhanced by consolidation, with increases in consolidation effective stress corresponding to increases in solute restriction as reflected by increases in membrane efficiency. However, the effect of consolidation on the membrane behavior of GCLs has not been studied. As a result, the purpose of this study was to evaluate the influence of consolidation effective stress, σ', on the membrane efficiency of a commercially available GCL containing sodium bentonite. The GCL evaluated in this study previously has been shown to possess semipermeable membrane behavior (Malusis and Shackelford, 2002a,b), but the influence of consolidation effective stress was not evaluated, primarily because the rigid-wall apparatus used in that study was not capable of allowing such an evaluation. Accordingly, the membrane behavior of the GCL evaluated in this study was based on the use of a flexible-wall membrane cell that allowed for control of the state of stress in the GCL specimens, thereby permitting the evaluation of the effect of σ' on ω. Thus, the results of this study represent the first attempt to quantify the potential effect of consolidation effective stress on the membrane behavior of a GCL.

2. Materials and experimental methods

2.1. Materials

The GCL tested in this study is the same as that used by Malusis and Shackelford (2002a,b) and is marketed commercially under the trade name Bentomat® (Colloid Environmental Technologies Company (CETCO), Hoffman Estates, Illinois, USA). The physical and chemical properties as well as the mineralogical composition of the bentonite portion of the GCL were reported by Malusis and Shackelford (2002a,b). In terms of mineralogy, the bentonite component of the GCL contained 71% smectite (montmorillonite), 7% mixed layer illite/smectite, 15% quartz, and 7% other minerals. The liquid limit (*LL*) and plastic limit (*PL*) measured in accordance with ASTM D4318 were reported as 478% and 39%, respectively, and the bentonite classified as a high plasticity clay (CH) based on the Unified Soil Classification System (ASTM D2487). The measured cation exchange capacity, *CEC*, was reported as 47.7 meq/100 g (= 47.7 $cmol_c$/kg), and ~53% of the exchange complex was reported as being comprised of exchangeable sodium (i.e., sodium bentonite). Further details regarding the physical and chemical properties of the bentonite in the GCL are provided by Malusis and Shackelford (2002a,b)

2.2. Flexible-wall membrane cell

The flexible-wall membrane cell and associated hydraulic control system described in detail by Kang and Shackelford (2009) were used in this study to measure the stress dependency of the membrane behavior of the GCL. A schematic of the flexible-wall cell is illustrated in Fig. 1. In brief, after assembling a specimen into the cell and applying the appropriate confining and back pressures to establish an initial effective stress, σ', source electrolyte solutions are circulated at the same, constant rate across the top and bottom of the specimen under closed-system conditions such that volume change within the system is prevented. In the case where the concentration of the source electrolyte solution circulated across the top of the specimen, C_{ot}, is greater than that being circulated across the bottom of the specimen, C_{ob} (i.e., $C_{ot} > C_{ob}$), and the specimen behaves as a semipermeable membrane, there is a tendency for establishment of a chemico-osmotic liquid flux, q_π, from the bottom to the top of the specimen (i.e., in the direction of increasing salt concentration). However, because the system is closed and stainless steel tubing is used for all connecting lines such that volume change is prevented, a chemico-osmotic pressure difference, ΔP, is established across the specimen to counteract this tendency for chemico-osmotic liquid flux. The magnitude of ΔP is measured using a differential transducer, and the measured value of ΔP is used to determine the membrane efficiency of the specimen. Further details of the flexible-wall cell are provided in Kang and Shackelford (2009), and the hydraulic control system is described in detail by Malusis et al. (2001).

The closed-system boundary conditions imposed in the measurement of the membrane efficiency in this study are not likely to be the same as those encountered in field applications,

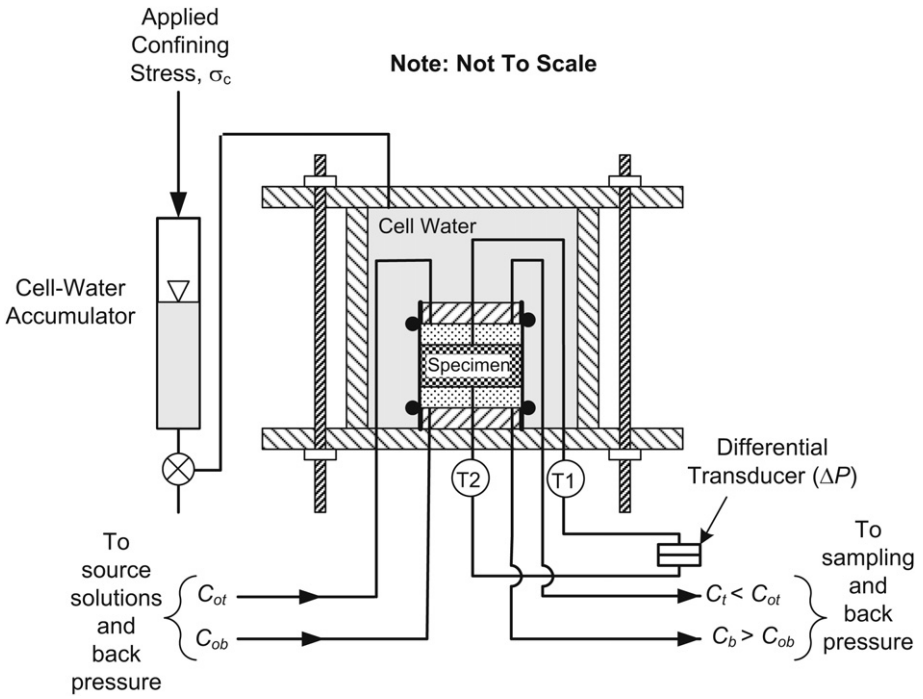

Fig. 1. Schematic diagram of flexible-wall cell used to measure membrane behavior (after Kang and Shackelford, 2009).

where open-system conditions are probable. However, the imposition of closed-system boundary conditions facilitates the laboratory measurement of the membrane behavior, as open-system conditions would require the measurement of the q_π resulting from establishing the concentration difference across the specimen. In this regard, closed-system conditions are more commonly used to measure membrane behavior than open-system conditions, because of the relative ease and greater accuracy in measuring ΔP under closed-system conditions relative to measuring q_π under open-system conditions, as the magnitudes of q_π can be small (Kang and Shackelford, 2009).

2.3. Specimen assembly and preparation

Specimen assembly and disassembly consisted of three stages: a flushing stage, a consolidation stage, and a membrane testing stage. The purpose of the flushing stage was to flush (leach) soluble salts from the pores of the bentonite in the GCL to enhance the likelihood that membrane behavior would be observed in the test specimens prior to consolidation and membrane testing. This flushing stage also was performed by Malusis and Shackelford (2002a,b) in their evaluation of the membrane behavior for the same GCL as used in this study, as well as in several other studies evaluating the membrane behavior of various clay soil barrier materials (e.g., see Malusis et al., 2001; Shackelford and Lee, 2003; Yeo et al., 2005; Henning et al., 2006; Kang and Shackelford, 2009).

For the flushing stage, circular specimens of the GCL with nominal diameters of 102 mm were cut from a larger GCL sheet and placed on the base pedestal in a flexible-wall permeameter (Daniel, 1994). Each GCL specimen was subjected to an effective stress, σ', of 34.5 kPa (5 psi) under 172 kPa (25 psi) back pressure before permeation with de-ionized water (DIW) to saturate the specimen, remove the excess soluble salts, and measure the initial hydraulic conductivity, k.

After completion of the flushing stage, the GCL specimen was transferred to the flexible-wall membrane cell shown schematically in Fig. 1, and the final stress conditions imposed during the flushing stage were re-established such that σ' was 34.5 kPa (5 psi) under a back pressure of 172 kPa (25 psi). Following re-establishment of the initial value of σ' of 34.5 kPa (5 psi), three of the four GCL specimens were consolidated further to final values of σ' of 103 kPa (15 psi), 172 kPa (25 psi), 241 kPa (35 psi) by increasing only the cell pressure in a single loading step (i.e., while maintaining the back pressure of 172 kPa (25 psi)). During this consolidation procedure, volume changes were monitored versus time by measuring changes in the air–water interface within the cell-water accumulator attached to the flexible-wall cell (Fig. 1), and changes in the specimen height were determined using a telescope sighted to markings located on the specimen membrane located within the flexible-wall cell. These measured changes in volume and height were used to evaluate the consolidation behavior of the specimens in the traditional manner via time–strain curves (Kang, 2008; Kang and Shackelford, 2010). Thus, four GCL specimens representing four different initial values of σ' (i.e., 34.5 kPa (5 psi), 103 kPa (15 psi), 172 kPa (25 psi), 241 kPa (35 psi)) were prepared for membrane testing.

2.4. Membrane testing procedures and program

The same membrane testing procedures as described in detail by Kang and Shackelford (2009) were used in this study. At the end of consolidation, the drainage lines were closed, and the membrane stage of the test started by circulating DIW through the top and bottom boundaries of the specimen at a circulation rate of 4.2×10^{-10} m^3/s for approximately 7 d to establish a steady baseline pressure difference. This circulation rate has been proven to be sufficiently fast to maintain reasonably constant concentration boundaries (Malusis et al., 2001). The membrane efficiency measurements then were initiated by circulating solutions of potassium chloride (KCl) with different initial source concentrations through the top piston (i.e., $C_{ot} > 0$), while continuing circulation of DIW in the base pedestal (i.e., $C_{ob} = 0$).

Membrane testing consisted of multiple-stage (MS) membrane tests, with each MS test including five sequential stages in which

chemico-osmotic pressure differences corresponding to five different source KCl solutions, (i.e., C_{ot} = 3.9, 6.0, 8.7, 20, and 47 mM) were measured across the same GCL specimen. These five different source KCl solutions were the same as those previously used by Malusis and Shackelford (2002a,b) for the same GCL and circulation control system, but with a rigid-wall membrane cell instead of the flexible-wall membrane cell used in this study. Each stage lasted seven days, which was sufficient in all cases to achieve a steady chemico-osmotic pressure difference, $-\Delta P$ (>0, since the positive *x*-direction is assumed downward from the top of the specimen), across the specimen, as well as steady values for the electrical conductivity, *EC*, in samples recovered from the circulations outflows across the top (EC_{top}) and bottom (EC_{bottom}). Thus, the time required to complete a single MS test with five such circulation stages was 35 d (i.e., excluding the durations for the flushing and consolidation stages).

As described by Kang and Shackelford (2009), $-\Delta P$ was measured both directly and indirectly for comparison, i.e., to ensure precision in results. The direct measurement of $-\Delta P$ was obtained using a differential pressure transducer (Model DP15, Validyne Engineering Sales Corp., Northridge, California, USA) connected to the top and bottom boundaries of the specimen (Fig. 1). The indirect measurement of $-\Delta P$ was obtained as the difference between the boundary pressures at the top (u_{top}) and the bottom (u_{bottom}) of the specimen (i.e., $-\Delta u = u_{top} - u_{bottom}$) measured independently using two in-line pressure transducers (Model PX181-100G5V, OMEGA, Stamford, Connecticut, USA) denoted as T1 and T2, respectively, in Fig. 1.

The concentrations of KCl in samples of the circulation outflows from the top and bottom boundaries of the specimens, C_t and C_b, respectively, were estimated based on a calibration curve established between KCl concentration and the measured values for *EC* (i.e., EC_{top} and EC_{bottom}). Such estimated concentrations are based implicitly on the assumption that the only contributions to the *EC* in the circulation outflows from the specimen boundaries were due solely to the chloride (Cl^-) and potassium (K^+). This assumption was expected to have been reasonably accurate since the GCL specimens were permeated with DIW during the flushing stage prior to membrane testing to remove excess soluble salts from the pore water of the specimens. Because KCl is expected to diffuse into the specimen from the top boundary during circulation, C_t should be less than C_{ot}, whereas C_b should be greater than C_{ob} due to diffusion of salts from the specimen into the circulation boundary at the bottom of the specimen (Malusis et al., 2001; Kang and Shackelford, 2009).

Although the membrane testing stage was performed under closed-system (undrained) boundary conditions, Kang and Shackelford (2009) noted relatively small, daily volume changes ($\leq\pm$0.6%) in their specimens during the membrane testing stage. These small volumes changes were attributed to drainage of pore liquid from the specimens during brief periods ($\leq$2 min) when the drainage lines were momentarily left open for daily refilling of inflow solutions and sampling of outflow solutions. After the completion of these brief refilling/sampling periods, the drainage lines were closed during the subsequent, membrane measurement periods which lasted ~24 h. Thus, although some changes in specimen volume were anticipated during the membrane testing stage, the assumption of undrained conditions existing during the actual periods of measurement of membrane behavior were still valid.

Since the cell and back pressures were constant during the membrane stage of testing, the drainage during the refilling/sampling periods was attributed to an increase in effective stress resulting from a decrease in the repulsive electrical forces relative to the adsorptive forces between individual soil particles (i.e., so-called *R–A* effect), due to an increase in salt (KCl) concentration in the pore water of the GCL specimens (Kang and Shackelford, 2009). Such an increase in KCl concentration in the specimen pores results from diffusion of KCl from the top boundary into the specimen in the case of imperfect semipermeable membrane behavior (e.g., see Malusis et al., 2001; Shackelford and Lee, 2003). This phenomenon has been referred to as osmotic consolidation (e.g., Mitchell et al., 1973; Barbour and Fredlund, 1989; Di Maio, 1996). As a result of these considerations, volume changes also were recorded during the membrane testing stage via the cell-water accumulator (Fig. 1).

2.5. Calculation of membrane efficiency

Under closed-system boundary conditions such as those imposed in this study, the membrane efficiency coefficient, ω, is defined as follows (Groenevelt and Elrick, 1976; Malusis et al., 2001):

$$\omega = \frac{\Delta P}{\Delta \pi} \tag{1}$$

where ΔP (<0) is the measured chemico-osmotic pressure difference induced across the specimen as a result of prohibiting chemico-osmotic flux of solution, and $\Delta\pi$ (<0) is the theoretical chemico-osmotic pressure difference across an "ideal" semipermeable membrane (i.e., $\omega = 1$) subjected to an applied difference in solute (electrolyte) concentration (e.g., Olsen et al., 1990). The value of $\Delta\pi$ in Eq. (1) can be calculated in accordance with the van't Hoff expression in terms of either the source concentrations of KCl in the circulation inflows across the bottom and top of the specimens, or the average of the boundary salt concentrations across the top and bottom of the specimens, as follows (Kang and Shackelford, 2009):

$$\Delta\pi = \nu RT\Delta C = \nu RT(C_2 - C_1) \tag{2}$$

where ν is the number of ions per molecule of the salt, R is the universal gas constant [8.314 J mol^{-1} K^{-1}], T is the absolute temperature (K), C is the salt concentration (M), and subscripts 1 and 2 represent the individual compartments on either side of the soil specimen. For example, for 1:1 electrolyte solutions (e.g., NaCl, KCl), ν = 2 in Eq. (2), whereas for 2:1 electrolyte solutions (e.g., $CaCl_2$), ν = 3 in Eq. (2). The resulting membrane efficiency coefficient in terms of the source KCl concentrations, designated as ω_o, is given as follows:

$$\omega_o = \frac{\Delta P}{\Delta\pi}\bigg|_o = \frac{\Delta P}{\Delta\pi_o} = \frac{\Delta P}{\nu RT\Delta C_o} = \frac{\Delta P}{\nu RT(C_{ob} - C_{ot})} = \frac{\Delta P}{-\nu RTC_{ot}} \tag{3}$$

where T is 293 K in this study corresponding to 20 °C, and C_{ot} (>0) and C_{ob} (=0) are the initial concentrations of KCl (M) in the source solutions introduced across the top and bottom specimen boundaries, respectively. In terms of average KCl concentrations, the membrane efficiency coefficient, ω_{ave}, is given as follows:

$$\omega_{\text{ave}} = \frac{\Delta P}{\Delta\pi}\bigg|_{ave} = \frac{\Delta P}{\Delta\pi_{ave}} = \frac{\Delta P}{\nu RT\Delta C_{ave}} = \frac{\Delta P}{\nu RT\left(C_{b,ave} - C_{t,ave}\right)} \tag{4}$$

where $C_{t,ave}$ and $C_{b,ave}$ are the average KCl concentrations across the top and bottom of the specimen boundaries defined as follows:

$$C_{t,ave} = \frac{C_{\text{ot}} + C_t}{2}; \quad C_{b,ave} = \frac{C_{\text{ob}} + C_b}{2} \tag{5}$$

and C_b and C_t are the measured KCl concentrations (i.e., via calibration with *EC*) in the circulation outflows from the bottom and top of the specimen boundaries, respectively (see Fig. 1). Since

$C_{t,ave} < C_{ot}$ and $C_{b,ave} \geq C_{ob}$, the magnitude of $\Delta\pi_o$ will be greater than that of $\Delta\pi_{ave}$ such that, for the same measured value of ΔP, $\omega_o < \omega_{ave}$. Thus, membrane efficiencies based on source salt concentrations typically are more conservative (lower) than those based on average salt concentrations (Malusis et al., 2001). However, in the limit as the membrane efficiency approaches 100 percent, solutes cannot enter or exit the specimen, such that $C_{t,ave}$ approaches C_{ot}, $C_{b,ave}$ approaches C_{ob}, and ω_{ave} approaches ω_o (Kang and Shackelford, 2009).

3. Results

3.1. Specimen flushing and consolidation

The results of the flushing stage of the tests are shown in Fig. 2. As indicated in Fig. 2a, the four GCL specimens, designated as GCL1, GCL2, GCL3, GCL4, were permeated with DIW under an average effective stress of 34.5 kPa (5 psi) for periods ranging from 105 d to 209 d resulting in final *EC* values ranging from 16.9% to 41.7% of the source solution *EC*, or EC_o, of 56.1 mS/m for the 3.9 mM KCl source solution. The EC_o values for the other source solutions used in the study also are provided in Fig. 2a for comparison.

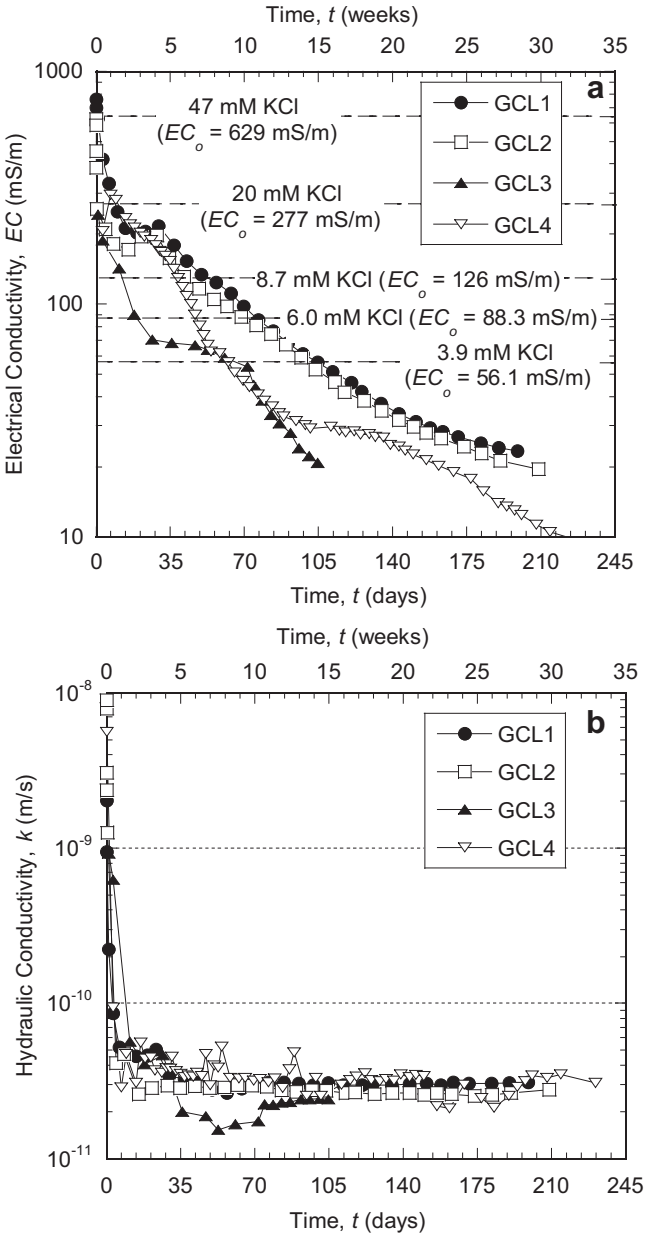

Fig. 2. Electrical conductivity (a) and hydraulic conductivity (b) versus elapsed time of permeation for specimens of a geosynthetic clay liner permeated with de-ionized water during flushing stage of test prior to consolidation.

As shown in Fig. 2b, despite somewhat initially erratic behavior, permeation with DIW eventually resulted in measured steady-state *k* values for specimens GCL1, GCL2, GCL3 and GCL4 of 3.06×10^{-11} m/s, 2.63×10^{-11} m/s, 2.41×10^{-11} m/s, and 3.34×10^{-11} m/s, respectively. These *k* values are representative of those typically measured for GCLs permeated with DIW in flexible-wall permeameters and similar effective stresses (e.g., see Daniel et al., 1997).

3.2. Electrical conductivity

The values for *EC* measured in the circulation outflows from the top (EC_{top}) and bottom (EC_{bottom}) boundaries during the membrane testing stage are shown in Fig. 3. These measured *EC* values reflect the boundary conditions imposed in the tests (Shackelford and Lee, 2003; Kang and Shackelford, 2009). For example, the increasing magnitude of EC_{top} upon replacing the DIW with the KCl solutions directly reflects the progressively greater increase in ionic strength of the KCl solutions resulting from the circulation of solutions with progressively higher KCl concentrations. The lower values for EC_{top} relative to the EC_o values for the source solutions (i.e., $EC_{top} < EC_o$), are consistent with the loss of solute mass from the source solutions due to solute diffusion into the specimens, whereas the eventual increase in the values of EC_{bottom} with time is consistent with the gain of solute mass in the bottom circulation outflow due to solute diffusion through the specimen. Finally, the leveling off of the values for both EC_{top} and EC_{bottom} during the 7-d periods applied for each stage of the test reflects the establishment of steady-state conditions with respect to *EC* in both the top and bottom boundaries.

3.3. Chemico-osmotic pressure difference

The temporal values in $-\Delta P$ (>0) measured by the differential pressure transducer (Fig. 1) as well as the differences between the pressures measured at the top and bottom boundaries of the specimen by the in-line transducers (T1 and T2 in Fig. 1), $-\Delta u$ ($= u_{top} - u_{bottom}$), are shown in Fig. 4. As expected, differences between $-\Delta u$ and $-\Delta P$ are virtually indistinguishable for all GCL specimens (i.e., $-\Delta u \approx -\Delta P$). The results shown in Fig. 4 also indicate that, whereas virtually no membrane behavior (i.e., $-\Delta P \approx 0$) was observed during circulation of DIW through both the top and bottom boundaries of the specimens, significant and sustained membrane behavior (i.e., $-\Delta P > 0$) occurred in both specimens virtually immediately upon replacing the DIW circulating through the top boundary with KCl solutions.

3.4. Membrane efficiencies

The temporal variations in the effective chemico-osmotic pressure differences, $-\Delta P_e$, for all four GCL specimens as well as the calculated membrane efficiencies based on both the initial source KCl concentrations and the average of the boundary KCl concentrations in accordance with Eqs. (3) and (4), respectively, are shown in Fig. 5. As described by Malusis et al. (2001), the values for $-\Delta P_e$ shown in Fig. 5a represent the net pressure differences equal to the measured values of $-\Delta P$ based on circulation with the KCl solutions minus the measured value of $-\Delta P$ based on circulation with DIW through both top and bottom boundaries at the beginning of the membrane testing stage, or $-\Delta P_e = -\Delta P_{KCl} - (-\Delta P_{DIW})$. In

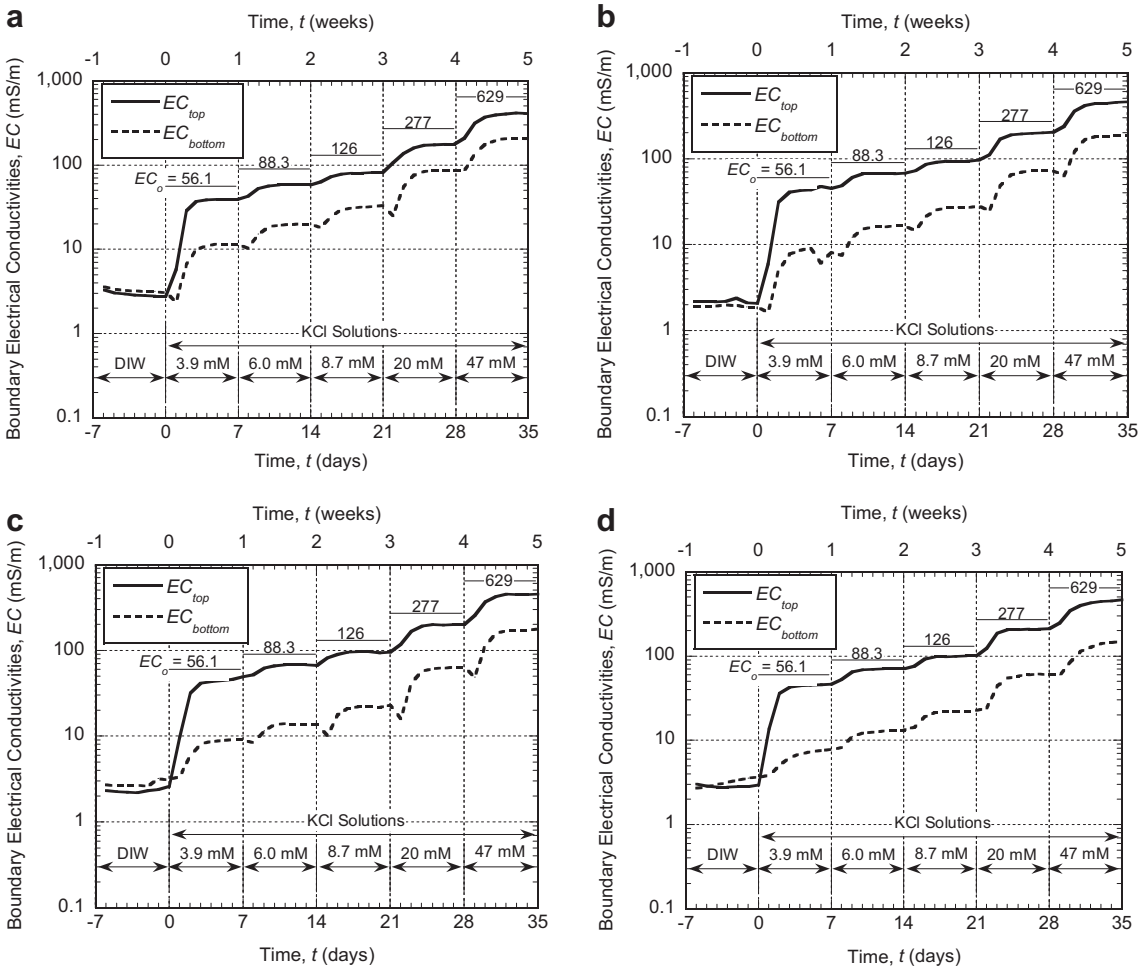

Fig. 3. Electrical conductivity values in circulation outflows from top and bottom boundaries of specimens of a geosynthetic clay liner consolidated to initial effective stresses of (a) 34.5 kPa (5 psi), (b) 103 kPa (15 psi), (c) 172 kPa (25 psi), and (d) 241 kPa (35 psi) as a function of elapsed time after salt (KCl) circulation.

calculating $-\Delta P_e$, the maximum value of $-\Delta P_{DIW}$ occurring during DIW circulation was used to provide conservative (low) estimates for $-\Delta P_e$ and, therefore, low estimates of ω.

As shown in Fig. 5a, three observations are apparent in the temporal trends in $-\Delta P_e$ with increasing source KCl concentration, C_{ot}, being circulated across the top boundary of a specimen. First, there was a tendency for a post-peak degradation in the magnitude of $-\Delta P_e$ within a given stage of a test. Second, the buildup in $-\Delta P_e$ between subsequent stages of a test tended to diminish with increasing C_{ot} such that the magnitude of $-\Delta P_e$ at the higher KCl concentrations was actually lower than that at the lower KCl concentrations. Third, the tendency for a post-peak degradation in $-\Delta P_e$ within a given stage of testing and the extent to which $-\Delta P_e$ diminished with increasing C_{ot} also tended to be greater with decreasing consolidation effective stress. Both the decrease in magnitude of $-\Delta P_e$ with increasing C_{ot} and the tendency for post-peak degradation in $-\Delta P_e$ previously have been observed in membrane tests involving the same GCL, and have been attributed to collapse of the diffuse-double layers (DDLs) associated with individual particles of the bentonite due to an increase in the concentration of KCl in the pores resulting from diffusion (e.g., see Malusis et al., 2001; Malusis and Shackelford, 2002a; Shackelford and Lee, 2003). However, unlike previous studies, the results shown in Fig. 5a indicate that the adverse impact of increasing C_{ot} on the magnitude of $-\Delta P_e$ can be assuaged to some extent by increasing the effective stress in the specimen.

As shown in Fig. 5b and c, the values of ω tended to decrease with increasing KCl concentration, which again is consistent with previous results based on rigid-wall cells that attributed decreasing ω with increasing salt concentration to a progressively greater collapse of the DDLs surrounding individual clay particles, resulting in larger pores and correspondingly less restriction of solutes (e.g., Malusis et al., 2001; Malusis and Shackelford, 2002a; Shackelford et al., 2003). Also, the values of ω were relatively constant over any interval of time corresponding to a given KCl concentration, implying that steady-state conditions were achieved during the 7-d circulation periods. Finally, for a given stage of testing (i.e., given C_{ot}), the values of ω tended to decrease with decreasing consolidation effective stress, as expected.

3.5. Volume changes

As previously noted, volume changes were recorded during the membrane testing stage via the cell-wall accumulator (Fig. 1) as a check on the assumption of undrained conditions. Incremental volume changes, ΔV, of $\pm$0.36 mL, $\pm$0.33 mL, $\pm$0.24 mL, $\pm$0.47 mL were recorded during the membrane testing stage for the GCL specimens consolidated to effective stresses of 34.5 kPa (5 psi), 103 kPa (15 psi), 172 kPa (25 psi), and 241 kPa (35 psi), respectively, resulting in respective cumulative volume changes, $\Sigma(\Delta V)$, of $-$5.98, $-$2.33, $-$1.95, and $-$5.12 mL. As previously described, even though volume change was prevented from occurring during the

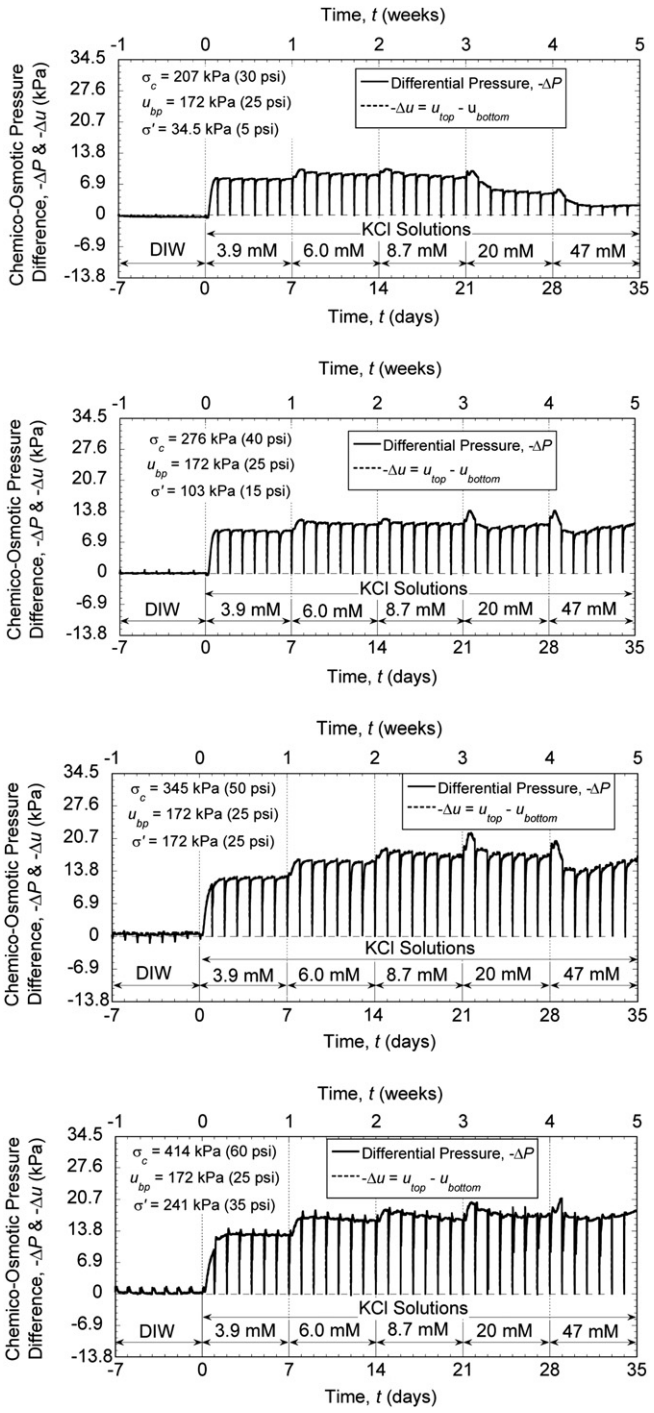

Fig. 4. Measured chemico-osmotic pressure differences across specimens of a geosynthetic clay liner consolidated to different initial effective stresses, σ', as a function of elapsed time after circulation of salt (KCl) solutions (σ_c = cell pressure, u_{bp} = back pressure).

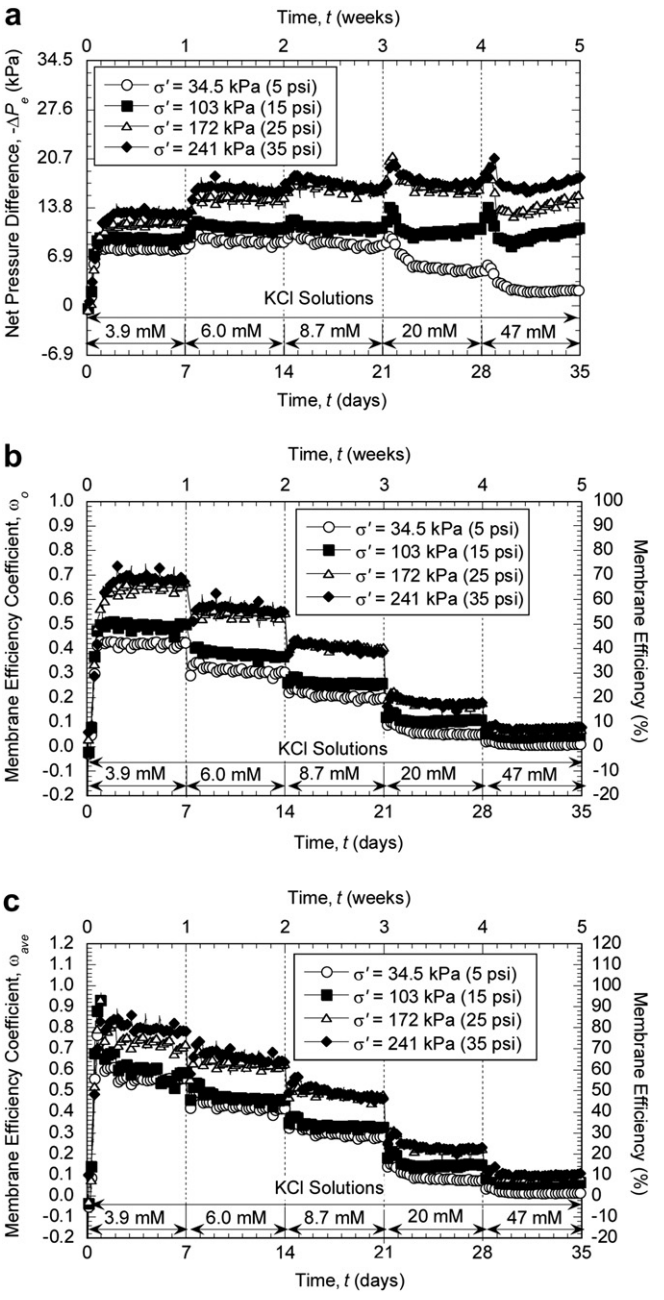

Fig. 5. Temporal variations in (a) induced effective (net) pressure differences and in measured membrane efficiencies based on (b) initial salt (KCl) concentration differences (ω_o) and (c) average salt concentration differences (ω_{ave}) across specimens of a geosynthetic clay liner as a function of consolidation effective stress, σ'.

periods of actual measurement of the membrane efficiency of the GCL specimens (i.e., during KCl circulation between sampling/refilling periods), some volume change did occur as a result of the sampling/refilling procedure and the desire to re-establish the reference (back) pressure before each daily circulation event. The resulting volume changes that did occur tended to be relatively low ($\leq -7.9\%$), and the resulting changes in the bulk specimen porosities resulting from these volumes changes tended to be relatively minor (see Table 2). Although the magnitude of the impact of these volume changes on the measured membrane efficiencies cannot be quantified, a decreasing specimen volume results in decreasing pore (void) space, which would be expected to increase solute restriction and, therefore, increase membrane efficiency.

4. Discussion

4.1. Effect of consolidation effective stress on steady-state membrane efficiency

The final, or steady-state, membrane efficiencies, $\omega_{o,ss}$ and $\omega_{ave,ss}$, based on Eqs. 3 and 4 along with the values of $-\Delta P_e$, $-\Delta\pi_o$, and $-\Delta\pi_{ave}$ used to calculate $\omega_{o,ss}$ and $\omega_{ave,ss}$, are summarized in

Table 1
Results of multi-stage membrane testing for specimens of the geosynthetic clay liner at each consolidation effective stress.

Effective stress, σ' [kPa (psi)]	KCl source concentration, C_{ot} (mM)	Differences in chemico-osmotic pressures[a] (kPa)			Membrane efficiency coefficients at steady state	
		$-\Delta P_e$	$-\Delta\pi_o$	$-\Delta\pi_{ave}$	$\omega_{o,ss}$ $(=\Delta P_e/\Delta\pi_o)$	$\omega_{ave,ss}$ $(=\Delta P_e/\Delta\pi_{ave})$
34.5 (5)	3.9	8.117	19.011	14.472	0.427	0.561
	6.0	9.007	29.247	21.556	0.308	0.418
	8.7	8.572	42.408	29.978	0.202	0.286
	20.0	4.903	97.490	64.776	0.050	0.076
	47.0	2.290	229.101	151.017	0.010	0.015
103 (15)	3.9	9.476	19.011	16.214	0.498	0.584
	6.0	10.966	29.247	23.787	0.375	0.461
	8.7	11.034	42.408	33.678	0.260	0.328
	20.0	11.028	97.490	72.520	0.113	0.152
	47.0	11.159	229.101	164.448	0.049	0.068
172 (25)	3.9	12.062	19.011	16.781	0.634	0.719
	6.0	15.241	29.247	24.287	0.521	0.628
	8.7	16.552	42.408	34.202	0.390	0.484
	20.0	16.634	97.490	73.531	0.171	0.226
	47.0	16.131	229.101	164.990	0.070	0.098
241 (35)	3.9	12.931	19.011	16.492	0.680	0.784
	6.0	15.952	29.247	25.112	0.545	0.635
	8.7	16.234	42.408	35.375	0.383	0.459
	20.0	17.593	97.490	76.384	0.180	0.230
	47.0	18.200	229.101	172.085	0.079	0.106

[a] $-\Delta P_e$ = effective or net chemico-osmotic pressure difference measured across specimen at steady state; $-\Delta\pi_o$ = theoretical chemico-osmotic maximum pressure difference based on difference in initial (source) concentrations; $-\Delta\pi_{ave}$ = theoretical maximum chemico-osmotic pressure difference based on difference in average boundary concentrations at steady state.

Table 1. The measured values of $\omega_{o,ss}$ and $\omega_{ave,ss}$ also are plotted as a function of σ' for different values of C_{ot} in Fig. 6a and b, respectively. As previously indicated, both $\omega_{o,ss}$ and $\omega_{ave,ss}$ based on a given C_{ot} tend to increase with increasing σ' and a given C_{ot}. However, the increase in $\omega_{o,ss}$ and $\omega_{ave,ss}$ tends to diminish with increasing σ', such that the trend in $\omega_{o,ss}$ or $\omega_{ave,ss}$ with increasing σ' appears to be asymptotic. A similar asymptotic behavior in the hydraulic conductivity of GCLs to water with increasing static (effective) confining stress was observed by Petrov et al. (1997). Also, the value of σ' at which such an asymptotic value of $\omega_{o,ss}$ or $\omega_{ave,ss}$ would be achieved appears to decrease with increasing C_{ot}. For example, the differences in $\omega_{o,ss}$ between σ' of 241 kPa (35 psi) and σ' of 172 kPa (25 psi), or $\Delta\omega_{o,ss}$, are 0.046, 0.024, −0.007, 0.009 and 0.009 for values of C_{ot} of 3.9, 6.0, 8.7, 20, and 47 mM KCl, respectively. However, the decrease in both $\omega_{o,ss}$ and $\omega_{ave,ss}$ with increase in σ' from 172 kPa (25 psi) to 241 kPa (35 psi) suggests some uncertainty in the trend. Also, this trend in difference in $\Delta\omega_{o,ss}$ with increasing σ' is not as clear in the case of $\omega_{ave,ss}$ (Fig. 6b). Finally, the fact that neither $\omega_{o,ss}$ nor $\omega_{ave,ss}$ achieves a constant value (i.e., $\Delta\omega_{o,ss} = 0$ or $\Delta\omega_{ave,ss} = 0$) within the ranges of σ' values evaluated in this study suggests that any such asymptotic value of $\omega_{o,ss}$ or $\omega_{ave,ss}$ would not be achieved until σ' was greater than 241 kPa (35 psi).

Table 2
Bulk porosities of GCL specimens during membrane testing.

Stage of test	Initial effective stress of specimen			
	34.5 kPa (5 psi)	103 kPa (15 psi)	172 kPa (25 psi)	241 kPa (35 psi)
After consolidation	0.81	0.80	0.77	0.71
After DIW circulation	0.81	0.80	0.77	0.70
After 3.9 mM KCl circulation	0.80	0.80	0.77	0.69
After 6.0 mM KCl circulation	0.80	0.80	0.77	0.68
After 8.7 mM KCl circulation	0.79	0.80	0.76	0.67
After 20 mM KCl circulation	0.79	0.80	0.76	0.66
After 47 mM KCl circulation	0.79	0.79	0.76	0.66

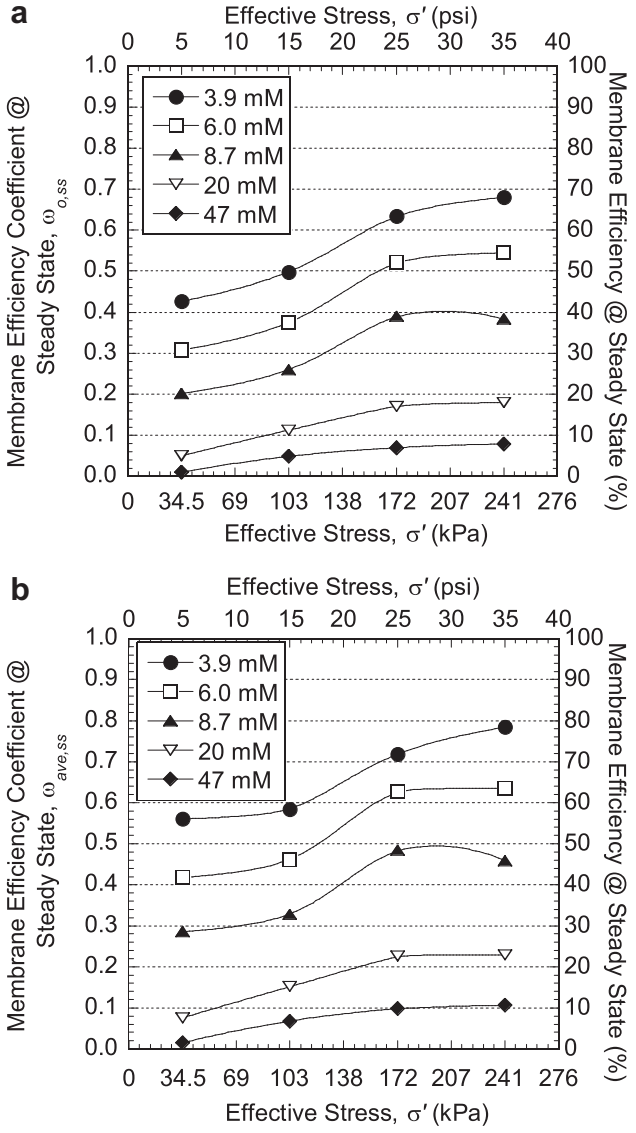

Fig. 6. Effect of consolidation effective stress on steady-state membrane efficiency coefficients based on (a) initial (source) boundary concentrations and (b) average boundary concentrations for specimens of a geosynthetic clay liner subjected to different source concentrations of potassium chloride (KCl).

The overall effect of σ' on the measured membrane efficiencies of the GCL is illustrated in Fig. 7, where the ratio of steady-state membrane efficiency coefficient at any value for σ', relative to that at σ' of 34.5 kPa (5 psi) is plotted as a function of σ'. As indicated in Fig. 7, the effect of increasing σ' on the measured membrane efficiency diminishes with decreasing C_{ot}. For example, as σ' increases from 34.5 kPa (5 psi) to 241 kPa (35 psi), the measured membrane efficiency increases by a factor ranging from 7.1 to 7.9 for C_{ot} of 47 mM KCl, from 3.0 to 3.6 for C_{ot} of 20 mM KCl, and from 1.4 to 1.9 for C_{ot} ranging from 8.7 to 3.9 mM KCl. In addition, the effect of increasing σ' is greater in terms of $\omega_{o,ss}$ versus $\omega_{ave,ss}$, primarily because the value of $\omega_{o,ss}$ at σ' of 34.5 kPa (5 psi) is lower than the value of $\omega_{ave,ss}$ at σ' of 34.5 kPa (5 psi). Thus, although higher values of C_{ot} generally result in lower measured membrane efficiencies, increasing σ' increases these lower membrane efficiencies at higher C_{ot}.

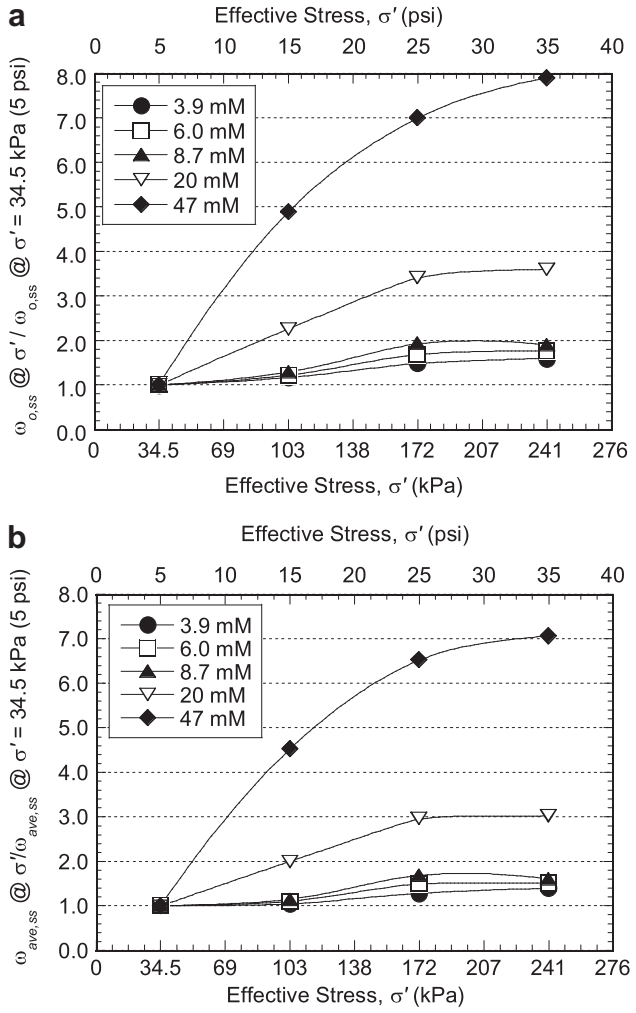

Fig. 7. Ratio of steady-state membrane efficiency coefficients at any consolidation effective stress, σ', to that at σ' of 34.5 kPa (5 psi) versus σ' for specimens of a geosynthetic clay liner subjected to different source concentrations of potassium chloride (KCl): (a) coefficients based on initial (source) boundary concentrations and (b) coefficients based on average boundary concentrations.

In general, the effect of increasing σ' in terms of mitigating the detrimental effect of increasing C_{ot} on the membrane efficiency of the GCL is consistent with the different mechanisms associated with the two factors. In the case of C_{ot}, the thickness of the diffuse-double layers decreases as C_{ot} increases, resulting in an increasingly greater portion of the pore space that is accessible for solute migration and an associated decrease in membrane efficiency. In contrast, the porosity of the soil decreases as σ' increases, such that the overall sizes of the individual pores within the soil decrease, thereby increasing the membrane efficiency. As illustrated by Shackelford et al. (2000), the effect of C_{ot} can occur at constant porosity (i.e., constant σ'), whereas the effect of σ' can occur at constant C_{ot}. Thus, decreasing the sizes of the pores via an increase in σ' can offset the detrimental effect of an increase in C_{ot} on the membrane efficiency of the GCL.

4.2. Effect of type of membrane cell on steady-state membrane efficiency

Values of the membrane efficiency measured in this study using the flexible-wall cell under closed-system boundary conditions are compared in Fig. 8 with values of the membrane efficiency

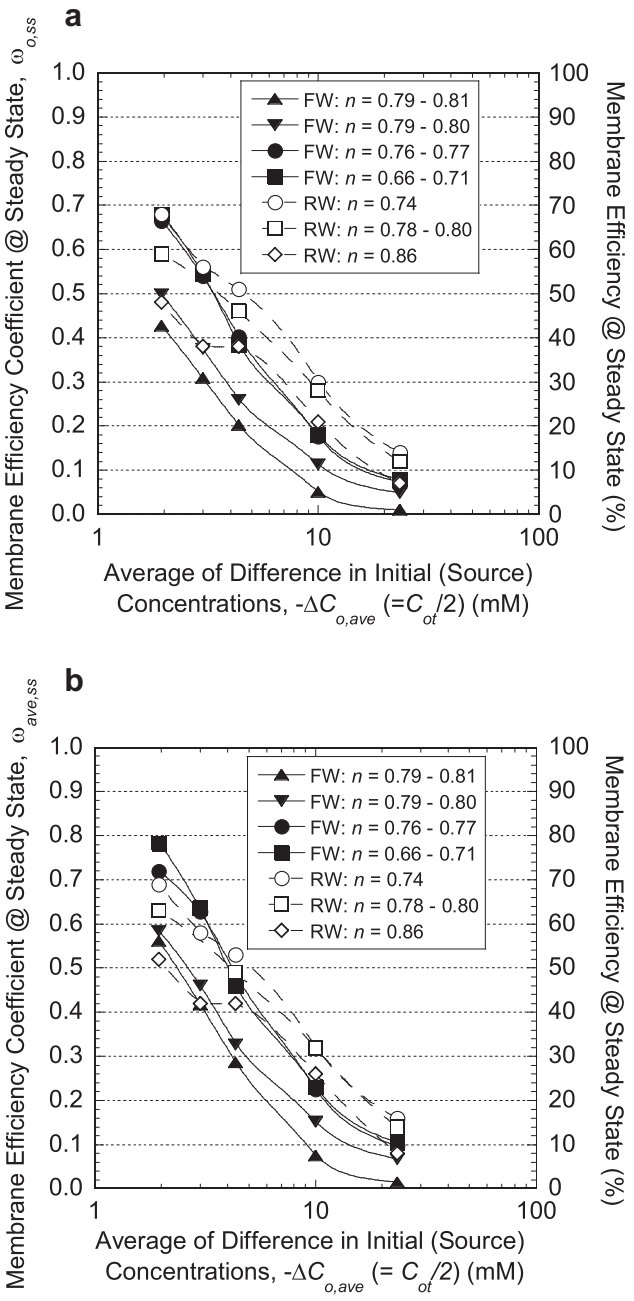

Fig. 8. Comparison of steady-state membrane efficiency coefficients based on (a) initial (source) boundary concentrations and (b) average boundary concentrations for specimens of a geosynthetic clay liner measured in this study using a flexible-wall (FW) cell versus those from Malusis and Shackelford (2002a) using a rigid-wall (RW) cell with different specimen bulk porosities, n.

previously reported by Malusis and Shackelford (2002a) for the same GCL and same source KCl concentrations measured using a rigid-wall cell under the same closed-system boundary conditions. Values of $\omega_{o,ss}$ and $\omega_{ave,ss}$ are plotted versus the average of the difference in initial (source) concentrations, or $-\Delta C_{o,ave}$, which is equivalent to half the source concentration, $C_{ot}/2$, to be consistent with the traditional approach for reporting such values (e.g., Kemper and Rollins, 1966; Malusis and Shackelford, 2002a).

As expected and previously discussed, the membrane efficiencies decrease with increasing KCl concentration regardless of whether the flexible-wall or rigid-wall cell is used in the measurement. However, at least two distinct differences in the membrane

efficiencies based on the flexible-wall cell versus those based on the rigid-wall cell are apparent. First, with some exceptions, the membrane efficiencies based on the flexible-wall cell generally are lower than those based on the rigid-wall cell at any given value of $-\Delta C_{o,ave}$. Second, whereas the membrane efficiency of the GCL based on the rigid-wall cell decreases essentially semi-log linearly with increasing $-\Delta C_{o,ave}$, the decrease in the membrane efficiency of the GCL based on the flexible-wall cell with increasing logarithm of $-\Delta C_{o,ave}$ is non-linear. The exact reasons for these differences in results based on the flexible-wall cell versus the rigid-wall cell are unknown, but likely can be attributed, in part, to differences in the stress conditions induced in the specimens, as well as the differences in the specimen preparation procedures, as discussed in detail by Kang and Shackelford (2009).

4.3. Effect of boundary salt concentrations on calculated membrane efficiencies

Values of the ratio of $\omega_{ave,ss}$ to $\omega_{o,ss}$, or $\omega_{ave,ss}/\omega_{o,ss}$, are shown as a function of C_{ot} in Fig. 9a and as a function of σ' in Fig. 9b. With respect to Fig. 9a, three observations are readily apparent. First, all of the values for $\omega_{ave,ss}/\omega_{o,ss}$ are greater than unity, as expected based on previous discussion, regardless of the value of σ' or C_{ot}. Second, for a given value of σ', $\omega_{ave,ss}/\omega_{o,ss}$ tends to increase approximately semi-log linearly with increasing C_{ot}. This trend is similar to that reported by Malusis and Shackelford (2002a) based on their membrane testing of the same GCL using a rigid-wall cell. Third, for a given C_{ot}, the value of $\omega_{ave,ss}/\omega_{o,ss}$ tends to increase with decreasing σ', although at C_{ot} of 3.9 mM KCl, the value for $\omega_{ave,ss}/\omega_{o,ss}$ at σ' of 241 kPa (35 psi) of 1.15 is slightly greater than the value for $\omega_{ave,ss}/\omega_{o,ss}$ at σ' of 172 kPa (25 psi) of 1.13. Overall, $\omega_{ave,ss}/\omega_{o,ss}$ ranges from 1.13 for C_{ot} of 3.9 mM KCl at σ' of 172 kPa (25 psi) to 1.52 for C_{ot} of 47 mM KCl at σ' of 34.5 kP as (5 psi). Thus, the difference between $\omega_{o,ss}$ based on Eq. (3) versus $\omega_{ave,ss}$ based on Eq. (4) tends to increase with increasing C_{ot}.

As indicated in Fig. 9b, for a given C_{ot}, the difference between $\omega_{o,ss}$ based on Eq. (3) versus $\omega_{ave,ss}$ based on Eq. (4) tends to decrease with increasing σ'. Thus, increasing the consolidation effective stress can diminish the effect of the boundary salt concentrations used in determining the membrane efficiency.

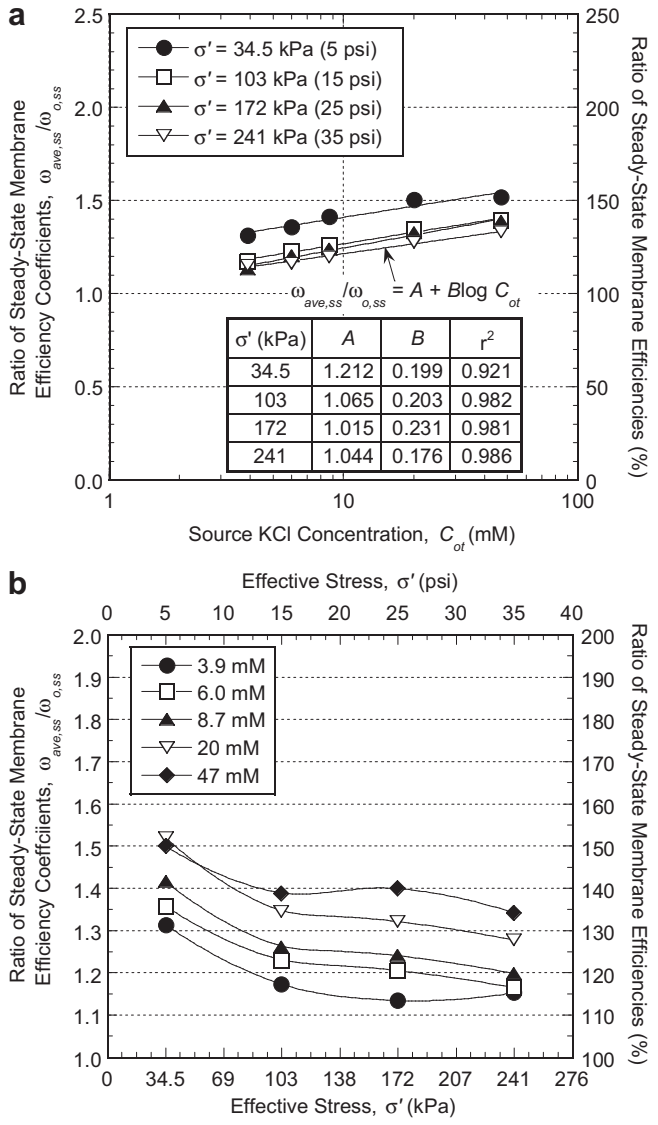

Fig. 9. Ratio of steady-state membrane efficiency based on average boundary concentrations ($\omega_{ave,ss}$) to that based on initial (source) boundary concentrations ($\omega_{o,ss}$) as a function of: (a) source KCl concentration, (b) consolidation effective stress.

4.4. Practical significance of results

The results of this study not only support the results of previous studies indicating that GCLs can behave as semipermeable membranes, but also indicate that the existence of such membrane behavior in GCLs can be enhanced by consolidation. The practical significance of these findings can be illustrated with the aid of a simplified example analysis showing the influence of chemico-osmosis due to membrane behavior on the total liquid flux through a GCL used as a containment barrier, as illustrated schematically in Fig. 10a. The scenario depicted in Fig. 10a may be representative of surface impoundment where the porous confining layer is assumed to offer negligible hydraulic resistance and the underlying subgrade soil maintains a zero concentration boundary, for example, via drainage.

In general, the total liquid flux through a soil that behaves as a semipermeable membrane, q, at steady state is the sum of a hydraulic component of liquid flux, q_h, in response to the difference in total hydraulic head in accordance with Darcy's law, and a chemico-osmotic component of liquid flux, q_π, in response to a difference in solute concentration, or $q = q_h + q_\pi$. (e.g., Barbour and Fredlund, 1989; Shackelford et al., 2001; Malusis et al., 2003). As a result, the contribution of the chemico-osmotic component of liquid flux to the total liquid flux can be ascertained by normalizing the total liquid flux, q, with respect to the hydraulic component of liquid flux, q_h, or q/q_h, as follows (e.g., Yeo et al., 2005; Henning et al., 2006):

$$\frac{q}{q_h} = \frac{q_h + q_\pi}{q_h} = 1 + \frac{q_\pi}{q_h} = 1 - \left(\frac{\omega \Delta \pi}{\gamma_w \Delta h}\right) \tag{6}$$

where γ_w = the unit weight of water (i.e., 9.81 kN/m^3 assuming dilute solutions), Δh = the total hydraulic head loss across the barrier, and all other parameters are as previously defined. Note that q_h is assumed to be in the positive x-direction as indicated in Fig. 10a, the value of Δh in Eq. (6) will be negative, since the final hydraulic head at the bottom of the GCL (h_f) will be less than the initial hydraulic head at the top of the GCL (h_i), or $\Delta h = h_f - h_i < 0$. Typically, for convenience, the pressure head between the barrier (GCL) and the underlying soil (subgrade) is assumed to be zero, such that $\Delta h = -(L + h_p)$, where L is the thickness of the barrier and h_p is the pressure head on containment side of the barrier resulting from the height of containment liquid, h_l, on the barrier (i.e., $h_p = h_l$).

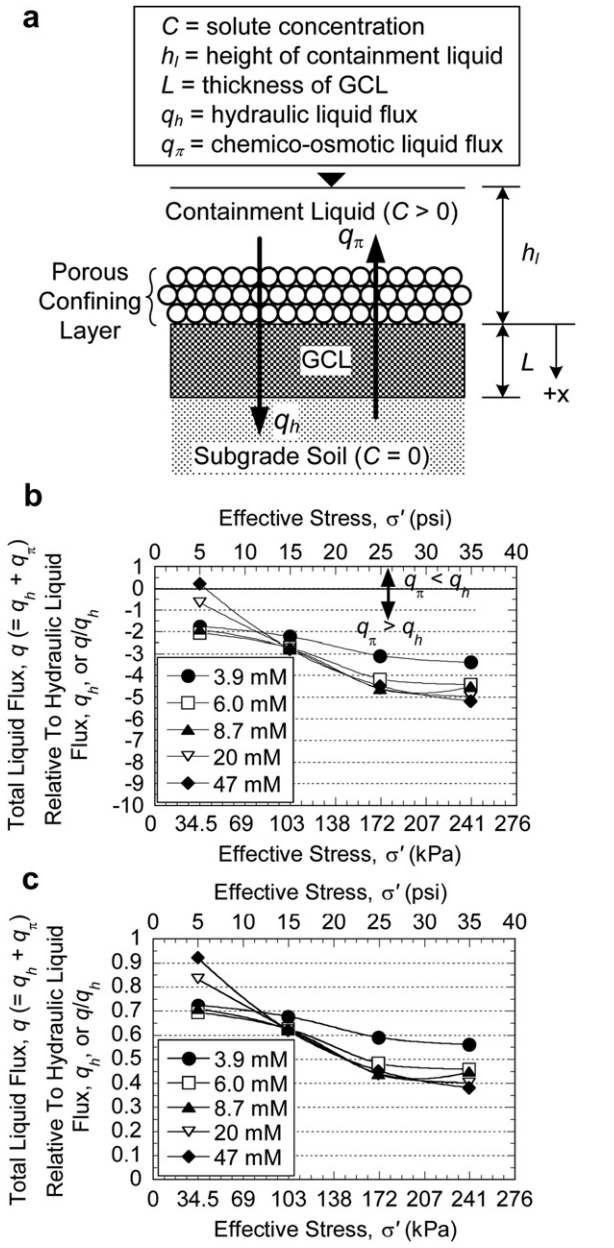

Fig. 10. Effect of chemico-osmotic counter flow through a geosynthetic clay liner (GCL) used as a containment barrier as a function of consolidation effective stress and KCl concentration in containment liquid: (a) simplified scenario; (b) h_l = 0.3 m; (c) h_l = 3.0 m.

In accordance with Eq. (1), the numerator in the second term in Eq. (6) represents the chemico-osmotic pressure difference, ΔP, such that Eq. (6) can be re-written as follows:

$$\frac{q}{q_h} = 1 - \left(\frac{\Delta P}{\gamma_w \Delta h}\right) = 1 - \left(\frac{\Delta h_\pi}{\Delta h}\right) \tag{7}$$

where $\Delta h_\pi (= \Delta P/\gamma_w)$ = the difference in chemico-osmotic pressure head across the barrier. The containment scenario considered herein is similar to that associated with the membrane testing conducted in this study (e.g., compare Figs. 1 and 10a), since the concentration of chemical constituents in the liquid on the containment side of the GCL (i.e., top) is greater than that on the outside of the barrier (i.e., bottom). As a result, ΔP in Eq. (7) also is negative, such that q_π is directed inward toward the containment liquid, thereby reducing the total liquid flux emanating from the containment side, q, via chemico-osmotic counter flow.

The results of the example analysis in the form of q/q_h based on Eq. (7) versus the consolidation effective stress, σ', are shown in Fig. 10b and c for heights of containment liquid, h_l, of 0.3 m and 3.0 m, respectively. The results of this study were included in the analysis by using the measured values for the effective chemico-osmotic pressure differences, ΔP_e (Table 1) for ΔP in Eq. (7). Also, because the values of h_l assumed in the analysis are much greater than the typical thicknesses of GCLs (i.e., $L \leq 10$ mm), or $h_l \gg L$, the magnitude of the head loss, Δh, in Eq. (7) was assumed to be equal to h_l, (i.e., $\Delta h = -(L + h_p) \approx -h_l$).

The results of the analysis shown in Fig. 10b,c indicate that the presence of membrane behavior in the GCL can significantly reduce the total liquid flux, q, emanating from the containment facility, and that the magnitude in the reduction of q due to q_π for a given h_l tends to increase with increasing σ', due to the general increase in GCL membrane efficiency with increasing σ'. For example, for the lower height of containment liquid of 0.3 m (Fig. 10b), q_π is greater in magnitude than q_h for all values of C_{ot} and σ' except $C_{ot} = 47$ mM KCl and $\sigma' = 34.5$ kPa (5 psi), such that no liquid flux emanates from the containment facility (i.e., $q/q_h < 0$). In the case where $C_{ot} = 47$ mM KCl and $\sigma' = 34.5$ kPa (5 psi) for $h_l = 0.3$ m, the combination of the highest source KCl concentration and lowest consolidation effective stress results in the lowest membrane efficiency for the GCL, such that some liquid flux emanates from the containment facility, but the amount emanating would be only 22.2% of that emanating in the absence of GCL membrane behavior (i.e., $q/q_h = 0.222$). However, as the height of containment liquid increases, the magnitude of q_h increases, such that the reduction in total liquid flux due to chemico-osmotic counter flow decreases. For example, for $C_{ot} = 3.9$ mM KCl and $\sigma' = 172$ kPa (25 psi), q/q_h increases from −3.099 to 0.590 as h_l increases from 0.3 m to 3.0 m, respectively.

The results shown in Fig. 10 are limited by the assumptions inherent in the analysis. Aside from those assumptions already noted, the assumption of a simple salt (KCl) as the sole constituents in the containment liquid, and the fact that the membrane efficiencies measured in this study were based on GCL specimens that were flushed by permeation with DIW prior to membrane testing probably are the most restrictive. In general, higher concentrations of ions in the containment liquid and/or in the pore water of the bentonite in the GCL likely would result not only in an increase in hydraulic conductivity of the GCL (Shackelford et al., 2000), but also in a reduced membrane efficiency (Shackelford and Lee, 2003; Mazzieri et al., 2010). However, an increase in the consolidation effective stress within the GCL not only can enhance the membrane behavior of the GCL as shown herein, but also can assist in resisting increases in the hydraulic conductivity of the GCL (Fernandez and Quigley, 1991; Petrov and Rowe, 1997; Shackelford et al., 2000). Nonetheless, the ability of the GCL to sustain any semipermeable membrane behavior in the long term is unknown at this time.

In contrast, the analysis upon which the results shown in Fig. 10 are based also does not include some additional advantages resulting from the potential existence of membrane behavior in the GCLs. For example, aside from potentially reducing the liquid flux emanating from a containment facility, solute restriction resulting from membrane behavior also can reduce the effective diffusion coefficient of solutes (e.g., Malusis and Shackelford, 2002b) and, therefore, the overall solute mass flux migrating through the GCL (e.g., Malusis and Shackelford, 2002b, 2004a,b; Manassero and Dominijanni, 2003; Malusis et al., 2003). Also, solute sieving or hyperfiltration can result in an increase in solute concentration on the inward side of containment barrier (e.g., Whitworth and Ghazifard, 2009), which would result in an increase in chemico-osmotic pressure head loss, Δh_π, and chemico-osmotic counter

flow, q_π with time. Nonetheless, the results of the simplified analysis conducted herein provide an indication that the existence of membrane behavior in GCLs can offer a potentially significant benefit to the containment function of the GCLs, and that this benefit can be enhanced with increasing consolidation effective stress, σ'.

Finally, as shown by Shackelford et al. (2003) and Shackelford (2011), the concentrations over which membrane behavior is evident, although seemingly dilute, can still range from four to six orders of magnitude greater than the regulated maximum contaminant levels (MCLs) of many of the primary inorganic contaminants of interest (e.g., As, Cd, Hg, Ni, Pb) and, therefore, are relevant for many practical applications. However, for some applications such as landfills involving leachates with significantly higher concentrations of multiple chemical constituents, the potential for any significant benefit resulting from membrane behavior in GCLs is likely to be problematic.

5. Summary and conclusions

The potential influence of consolidation effective stress, σ', on the membrane behavior of a GCL containing sodium bentonite was evaluated using a newly developed flexible-wall cell under closed-system boundary conditions. The GCL specimens were consolidated to final values for σ' of 34.5 kPa (5 psi), 103 kPa (15 psi), 172 kPa (25 psi), and 241 kPa (35 psi) prior to the start of membrane testing. Membrane testing consisted of multi-stage (MS) tests, whereby deionized water (DIW) was first circulated across both the bottom and the top of the specimens to establish a baseline pressure difference, $-\Delta P$ (>0), of the specimen, followed by circulation of source KCl solutions across the top of the specimen (while maintaining DIW circulation across the bottom of the specimen) with sequentially higher source concentrations, C_{ot}, of KCl to establish the salt concentration differences, $-\Delta C$ ($= C_{ot}$), required to evaluate the potential for membrane behavior.

The results indicated that the GCL behaved as a semipermeable membrane, with measured membrane efficiencies at steady state, ω_{ss}, based on the difference in initial (source) concentrations, $\omega_{o,ss}$, ranging from 0.01 ($\sigma' = 34.5$ kPa (5 psi)) at C_{ot} of 47 mM KCl to 0.68 ($\sigma' = 241$ kPa (35 psi)) at C_{ot} of 3.9 mM KCl, whereas ω_{ss} values based on the average of the difference in boundary concentrations, $\omega_{ave,ss}$, ranged from 0.02 ($\sigma' = 34.5$ kPa (5 psi)) at C_{ot} of 47 mM KCl to 0.78 ($\sigma' = 241$ kPa (35 psi)) at C_{ot} of 3.9 mM KCl. Also, for a given σ', both $\omega_{o,ss}$ and $\omega_{ave,ss}$ decreased with increasing C_{ot}, which is consistent with previous findings based on the use of a rigid-wall cell and attributable to progressively greater collapse of the electrostatic diffuse-double layers surrounding individual clay particles with increasing salt concentration in the pore water. In contrast, for a given C_{ot}, both $\omega_{o,ss}$ and $\omega_{ave,ss}$ increased with increasing σ', with the effect of increasing σ' on either $\omega_{o,ss}$ or $\omega_{ave,ss}$ increasing with increasing C_{ot}. The increase in $\omega_{o,ss}$ or $\omega_{ave,ss}$ with increasing σ' is consistent with lower porosities and more restrictive pores with increasing σ'.

Finally, $\omega_{ave,ss}$ was always greater than $\omega_{o,ss}$, with values for the ratio of $\omega_{ave,ss}$ to $\omega_{o,ss}$, or $\omega_{ave,ss}/\omega_{o,ss}$, increasing approximately semi-log linearly with increasing initial source concentration of KCl, C_{ot}, for a given σ', but decreasing non-linearly with increasing σ' for a given C_{ot}. Overall, $\omega_{ave,ss}/\omega_{o,ss}$ ranged from 1.13 for C_{ot} of 3.9 mM KCl at σ' of 172 kPa (25 psi) to 1.52 for C_{ot} of 47 mM KCl at σ' of 34.5 kP as (5 psi). Thus, the effect of the boundary salt concentrations used to determine the membrane efficiency of the GCL tended to increase with increasing C_{ot}, but decrease with increasing σ'.

Values of ω_{ss} measured in this study using a flexible-wall cell under closed-system boundary conditions were compared with values of ω_{ss} for the same GCL previously measured using a rigid-wall cell under the same closed-system boundary conditions. As expected, the membrane efficiencies decreased with increasing KCl concentration regardless of whether the flexible-wall or rigid-wall cell was used in the measurement.

The results of a simplified analysis based on the use of the GCL as a containment barrier illustrated significant reduction in the liquid flux emanating from the containment barrier due to the existence of membrane behavior in the GCL. The results indicated that the existence of chemico-osmotic counter flow not only could reduce the total liquid flux relative to that which would exist in the absence of membrane behavior, but also could prevent any liquid flux from emanating from the containment barrier in the case where the height of containment liquid was low (i.e., $h_l = 0.3$ m). Although restricted by the simplifying assumptions inherent in the analysis, including uncertainty in ability of the GCL to sustain the membrane behavior over the long term, the results indicate that the existence of membrane behavior in GCLs can offer a significant benefit to the containment function of the GCLs, and that this benefit can be enhanced with increasing consolidation effective stress, σ'.

Acknowledgments

Financial support for this study was provided by the U. S. National Science Foundation (NSF), Arlington, VA, under Grants CMS-0099430 entitled, “Membrane Behavior of Clay Soil Barrier Materials” and CMS-0624104 entitled, “Enhanced Clay Membrane Barriers for Sustainable Waste Containment”. The opinions expressed in this paper are solely those of the writers and are not necessarily consistent with the policies or opinions of the NSF.

References

Abduel-Naga, H.M., Bouazza, A., 2009. Numerical chracaterization of advective gas flow through GM/GCL composite liners having a circular defect in the geomembrane. Journal of Geotechnical and Geoenvironmental Engineering 135 (11), 1661–1671.

Abduel-Naga, H.M., Bouazza, A., 2010. A novel laboratory technique to determine the water retention curve of geosynthetic clay liners. Geosynthetics International 17 (5), 313–322.

ASTM D2487-06, 2010. Standard Practice for Classification of Soils for Engineering Purposes (Unified Soil Classification System). ASTM International, West Conshohocken, Pennsylvania.

ASTM D4318-05, 2010. Standard Test Methods for Liquid Limit, Plastic Limit, and Plasticity Index of Soils. ASTM International, West Conshohocken, Pennsylvania.

Barbour, S.L., Fredlund, D.G., 1989. Mechanisms of osmotic flow and volume change in clay soils. Canadian Geotechnical Journal 26 (4), 551–562.

Benson, C.H., Meer, S.R., 2009. Relative abundance of monovalent and divalent cations and the impact of desiccation on geosynthetic clay liners. Journal of Geotechnical and Geoenvironmental Engineering 135 (3), 349–358.

Benson, C.H., Thorstad, P.A., Jo, H.-Y., Rock, S.A., 2007. Hydraulic performance of geosynthetic clay liners in a landfill final cover. Journal of Geotechnical and Geoenvironmental Engineering 133 (7), 814–827.

Benson, C.H., Ören, A.H., Gates, W.P., 2010. Hydraulic conductivity of two geosynthetic clay liners permeated with hyperalkaline solution. Geotextiles and Geomembranes 28 (2), 206–218.

Boardman, B.T., Daniel, D.E., 1996. Hydraulic conductivity of desiccated geosynthetic clay liners. Journal of Geotechnical Engineering 122 (3), 204–208.

Bouazza, A., 2002. Geosynthetic clay liners. Geotextiles and Geomembranes 20 (1), 3–17.

Bouazza, A., Vangpaisal, T., 2007a. Gas permeability of GCLs: effect of poor distribution of needle-punched fibres. Geosynthetics International 14 (4), 248–252.

Bouazza, A., Vangpaisal, T., 2007b. Gas transmissivity at the interface of a geomembrane and geotextile cover of a partially hydrated geosynthetic clay liner. Geosynthetics International 14 (5), 316–319.

Daniel, D.E., 1994. State-of-the-art: laboratory hydraulic conductivity test for saturated soils. In: Daniel, D.E., Trautwein, S.J. (Eds.), Hydraulic Conductivity and Waste Contaminant Transport in Soil, STP 1142. ASTM, West Conshohoken, Pennsylvania, pp. 30–78.

Daniel, D.E., Shan, H.-Y., Anderson, J.D., 1993. Effects of partial wetting on the performance of the bentonite component of a geosynthetic clay liner. Geosynthetics '93. Industrial Fabrics Association International, St. Paul, Minnesota, USA, 3, pp. 1483–1496.

Daniel, D.E., Bowders, J.J., Gilbert, R.B., 1997. Laboratory hydraulic conductivity testing of GCLs in flexible-wall permeameters. In: Well, L. (Ed.), Testing and

Acceptance Criteria for Geosynthetic Clay Liners, STP 1308. ASTM, West Conshohocken, Pennsylvania, pp. 208–226.
Di Maio, C., 1996. Exposure of bentonite to salt solution: osmotic and mechanical effects. Géotechnique 46 (4), 695–707.
Dickinson, S., Brachman, R.W.I., 2010. Permeability and internal erosion of a GCL beneath coarse gravel. Geosynthetics International 17 (3), 112–123.
Dickinson, S., Brachman, R.W.I., Rowe, R.K., 2010. Thickness and hydraulic performance of geosynthetic clay liners overlying a geonet. Journal of Geotechnical and Geoenvironmental Engineering 136 (4), 552–561.
Estornell, P., Daniel, D.E., 1992. Hydraulic conductivity of three geosynthetic clay liners. Journal of Geotechnical Engineering 118 (10), 1592–1606.
Fernandez, F., Quigley, R.M., 1991. Controlling the destructive effects of clay – organic liquid interactions by application of effective stresses. Canadian Geotechnical Journal 28 (3), 388–398.
Fritz, S.J., 1986. Ideality of clay membranes in osmotic processes: a review. Clays and Clay Minerals 34 (2), 214–223.
Groenevelt, P.H., Elrick, D.E., 1976. Coupling phenomena in saturated homo-ionic montmorillonite: II. Theoretical. Soil Science Society of America Journal 40 (6), 820–823.
Guyonnet, D., Touze-Foltz, N., Norotte, V., Pothier, C., Didier, G., Gailhanou, H., Blanc, P., Warmont, F., 2009. Performance-based indicators for controlling geosynthetic clay liners in landfill applications. Geotextiles and Geomembranes 27 (5), 321–331.
Henning, J., Evans, J.C., Shackelford, C.D., 2006. Membrane behavior of two backfills from field-constructed soil-bentonite cutoff walls. Journal of Geotechnical and Geoenvironmental Engineering 132 (10), 243–249.
Hewitt, R.D., Daniel, D.E., 1997. Hydraulic conductivity of geosynthetic clay liners after freeze-thaw. Journal of Geotechnical and Geoenvironmental Engineering 123 (4), 305–313.
Hornsey, W.P., Scheirs, J., Gates, W.P., Bouazza, A., 2010. The impact of mining solutions/liquors on geosynthetics. Geotextiles and Geomembranes 28 (2), 191–198.
Kang, J.B., 2008. Membrane behavior of clay liner materials. PhD dissertation, Colorado State University, Fort Collins, Colorado.
Kang, J.B., Shackelford, C.D., 2009. Clay membrane testing using a flexible-wall cell under closed-system boundary conditions. Applied Clay Science 44 (1–2), 43–58.
Kang, J.-B., Shackelford, C.D., 2010. Consolidation of a geosynthetic clay liner under isotropic states of stress. Journal of Geotechnical and Geoenvironmental Engineering 136 (1), 253–259.
Kemper, W.D., Rollins, J.B., 1966. Osmotic efficiency coefficients across compacted clays. Soil Science Society of America Proceedings 30 (5), 529–534.
Koerner, R.M., 2005. Designing with Geosynthetics, fifth ed. Pearson Prentice Hall, Upper Saddle River, New Jersey.
Koerner, R.M., Daniel, D.E., 1995. A suggested methodology for assessing the technical equivalency of GCLs to CCLs. In: Koerner, R.M., Gartung, E., Zanzinger, H. (Eds.), Geosynthetic Clay Liners. Balkema, Rotterdam, pp. 73–98.
Lake, C.B., Cardenas, G., Goreham, V., Gagnon, G.A., 2007. Aluminum migration through a geosynthetic clay liner. Geosynthetics International 14 (4), 201–210.
Lange, K., Rowe, R.K., Jamieson, H., 2007. Metal retention in geosynthetic clay liners following permeation by different mining solutions. Geosynthetics International 14 (3), 178–187.
Lange, K., Rowe, R.K., Jamieson, H., 2009. Diffusion of metals in geosynthetic clay liners. Geosynthetics International 16 (1), 11–27.
Lange, K., Rowe, R.K., Jamieson, H., 2010. The potential role of geosynthetic clay liners in mine water treatment systems. Geotextiles and Geomembranes 28 (2), 199–205.
Lee, J.-Y., Shackelford, C.D., 2005. Impact of bentonite quality on hydraulic conductivity of geosynthetic clay liners. Journal of Geotechnical and Geoenvironmental Engineering 131 (1), 64–77.
Malusis, M.A., Shackelford, C.D., 2002a. Chemico-osmotic efficiency of a geosynthetic clay liner. Journal of Geotechnical and Geoenvironmental Engineering 128 (2), 97–106.
Malusis, M.A., Shackelford, C.D., 2002b. Coupling effects during steady-state solute diffusion through a semipermeable clay membrane. Environmental Science and Technology 36 (6), 1312–1319.
Malusis, M.A., Shackelford, C.D., 2004a. Explicit and implicit coupling during solute transport through clay membrane barriers. Journal of Contaminant Hydrology Amsterdam 72 (1–4), 259–285.
Malusis, M.A., Shackelford, C.D., 2004b. Predicting solute flux through a clay membrane barrier. Journal of Geotechnical and Geoenvironmental Engineering 130 (5), 477–487.
Malusis, M.A., Shackelford, C.D., Olsen, H.W., 2001. A laboratory apparatus to measure chemico-osmotic efficiency coefficients for clay soils. Geotechnical Testing Journal 24 (3), 229–242.
Malusis, M.A., Shackelford, C.D., Olsen, H.W., 2003. Flow and transport through clay membrane barriers. Engineering Geology 70 (3), 235–248.
Manassero, M., Dominijanni, A., 2003. Modelling the osmosis effect on solute migration through porous media. Géotechnique 53 (5), 481–492.
Mazzieri, F., Di Emidio, G., van Impe, P.O., 2010. Diffusion of calcium chloride in a modified bentonite: impact on osmotic efficiency and hydraulic conductivity. Clays and Clay Minerals 58 (3), 351–363.
Meer, S.R., Benson, C.H., 2007. Hydraulic conductivity of geosynthetic clay liners exhumed from landfill final covers. Journal of Geotechnical and Geoenvironmental Engineering 133 (5), 550–563.
Mendes, M.J.A., Pierson, P., Touze-Foltz, N., Mora, H., Palmeira, E.M., 2010a. Characterisation of permeability to gas of geosynthetic clay liners in unsaturated conditions. Geosynthetics International 17 (5), 344–354.
Mendes, M.J.A., Touze-Foltz, N., Palmeira, E.M., Pierson, P., 2010b. Influence of structural and material properties of GCLs on interface flow in composite liners due to geomembrane effects. Geosynthetics International 17 (1), 34–47.
Mitchel, J.K., Soga, K., 2005. Fundamentals of Soil Behavior, third ed. John Wiley and Sons, Inc., New York.
Mitchell, J.K., Greenberg, J.A., Witherspoon, P.A., 1973. Chemico-osmotic effects in fine-grained soils. Journal of the Soil Mechanics and Foundations Division 99 (SM 4), 307–322.
Olsen, H.W., 1969. Simultaneous fluxes of liquid and charge in saturated kaolinite. Soil Science Society of America Proceedings 33 (3), 338–344.
Olsen, H.W., Yearsley, E.N., Nelson, K.R., 1990. Chemico-osmosis versus Diffusion-osmosis. Transportation Research Record No. 1288. Transportation Research Board, Washington D.C., pp. 15–22.
Petrov, R.J., Rowe, R.K., 1997. Geosynthetic clay liner (GCL) – chemical compatibility by hydraulic conductivity testing and factors impacting its performance. Canadian Geotechnical Journal 34 (6), 863–885.
Petrov, R.J., Rowe, R.K., Quigley, R.M., 1997. Selected factors influencing GCL hydraulic conductivity. Journal of Geotechnical and Geoenvironmental Engineering 123 (8), 683–695.
Rossin-Poumier, S., Touze-Foltz, N., Pantet, A., 2011. Impact of synthetic leachate and permittivity of GCLs measured by filter press and oedopermeameter. Geotextiles and Geomembranes 29 (3), 211–221.
Rossin-Poumier, S., Touze-Foltz, N., Pantet, A., Monnet, P., Didier, G., Guyonnet, D., Morotte, V., 2010. Swell index, oedopermeametric, filter press and rheometric tests for identifying the qualification of bentonites used in GCLs. Geosynthetics International 17 (1), 1–11.
Scalia IV, J., Benson, C.H., 2010. Preferential flow in geosynthetic clay liners exhumed from final covers with composite barriers. Canadian Geotechnical Journal 47 (10), 1101–1111.
Scalia IV, J., Benson, C.H., 2011. Hydraulic conductivity of geosynthetic clay liners exhumed from landfill final covers with composite barriers. Journal of Geotechnical and Geoenvironmental Engineering 137 (1), 1–13.
Shackelford, C.D., 2011. Membrane behavior in geosynthetic clay liners. GeoFrontiers 2011, Dallas, TX, March 13-16, 2011, (CD-ROM). ASCE, Reston, VA, pp. 1961–1970.
Shackelford, C.D., Lee, J.-M., 2003. The destructive role of diffusion on clay membrane behavior. Clays and Clay Minerals 51 (2), 186–196.
Shackelford, C.D., Benson, C.H., Katsumi, T., Edil, T.B., Lin, L., 2000. Evaluating the hydraulic conductivity of GCLs permeated with non-standard liquids. Geotextiles and Geomembranes 18 (2–4), 133–161.
Shackelford, C.D., Malusis, M.A., Olsen, H.W., 2001. Clay membrane barriers for waste containment. Geotechnical News 19 (2), 39–43.
Shackelford, C.D., Malusis, M.A., Olsen, H.W., 2003. Clay membrane behavior for geoenvironmental containment. In: Culligan, P.J., Einstein, H.H., Whittle, A.J. (Eds.), Soil and Rock America Conference 2003 (Proceedings of the Joint 12th Panamerican Conference on Soil Mechanics and Geotechnical Engineering and the 39th U.S. Rock Mechanics Symposium), vol. 1. Verlag Glückauf GMBH, Essen, Germany, pp. 767–774.
Shackelford, C.D., Sevick, G.W., Eykholt, G.R., 2010. Hydraulic conductivity of geosynthetic clay liners to tailings impoundment solutions. Geotextiles and Geomembranes 28 (2), 149–162.
Whitworth, T.M., Ghazifard, A., 2009. Membrane effects in clay-lined inward gradient landfills. Applied Clay Science 43 (2), 248–252.
Yeo, S.-S., Shackelford, C.D., Evans, J.C., 2005. Membrane behavior of model soil-bentonite backfills. Journal of Geotechnical and Geoenvironmental Engineering 131 (4), 418–429.